International Journal of Biological Macromolecules 319 (2025) 145570

Contents lists available at ScienceDirect

International Journal of Biological Macromolecules

journal homepage: www.elsevier.com/locate/ijbiomac

Elucidating the modes of incorporation of the ferulic acid amides feruloyltyramine and feruloyloctopamine into the lignin-suberin fraction of potato periderms

José C. del Río [a,*], John Ralph [b,c], José J. Benítez [d], Susana Guzman-Puyol [e], José A. Heredia-Guerrero [e], Jorge Rencoret [a]

[a] Instituto de Recursos Naturales y Agrobiología de Sevilla, CSIC, Avda. Reina Mercedes, 10, 41012 Seville, Spain
[b] Department of Energy Great Lakes Bioenergy Research Center, the Wisconsin Energy Institute, University of Wisconsin-Madison, Madison, WI 53726, USA
[c] Department of Biochemistry, University of Wisconsin-Madison, Madison, WI 53706, USA
[d] Instituto de Ciencia de Materiales de Sevilla, Centro Mixto CSIC-Universidad de Sevilla, Calle Americo Vespucio 49, Isla de la Cartuja, Sevilla 41092, Spain
[e] Instituto de Hortofruticultura Subtropical y Mediterránea La Mayora, Consejo Superior de Investigaciones Científicas-Universidad de Málaga (IHSM, CSIC-UMA), Bulevar Louis Pasteur 49, 29010 Malaga, Spain

ARTICLE INFO

Keywords:
Potato periderm
Lignin
Suberin
Feruloyltyramine
Feruloyloctopamine
DFRC
NMR

ABSTRACT

Ferulic acid amides are naturally present in the cell walls of potato (*Solanum tuberosum*) periderms. In this study, we investigated their modes of incorporation into the periderm cell wall polymers. A lignin/suberin-enriched fraction was isolated and analyzed by GPC, DFRC, and 2D-NMR. The analyses revealed that the lignin domain of this fraction was predominantly composed of G-lignin units, with an H:G:S ratio of 2:70:28 (S/G ratio of 0.40). More importantly, the data also indicated the presence of two ferulic acid amides, feruloyltyramine and feruloyloctopamine, that are incorporated into the lignin/suberin structure of potato periderms through a variety of linkages, including 8–*O*–4′ and 4–*O*–β′ ether linkages, as well as 8–5′ linkages forming a phenylcoumaran structure involving the ferulate moiety. Although the phenolic groups of the tyramine and octopamine moieties could theoretically undergo oxidation, potentially creating additional sites for radical coupling, our research indicates that these groups remain predominantly as free phenolic entities that do not participate in radical coupling. On the other hand, all the phenolic groups of the ferulate moieties are bound through ether linkages reinforcing the conclusion that the feruloyltyramine and feruloyloctopamine moieties are linked to lignin/suberin within the cell wall via radical coupling reactions.

1. Introduction

Lignin is an aromatic polymer unique to vascular plants that provides essential structural support, rigidity, and defense against pathogens. Its synthesis is primarily driven by the oxidative radical coupling of three monolignols, *p*-coumaryl, coniferyl, and sinapyl alcohols, which differ in their degrees of methoxylation, and that are derived from the phenylpropanoid biosynthetic pathway [1–5]. Once synthesized, these monolignols are transported to, or simply diffuse to, the plant cell walls where they are oxidized via laccases and peroxidases generating free radicals that undergo combinatorial coupling reactions, resulting in a lignin polymer with a heterogeneous and irregular structure that contributes to the recalcitrance and resistance of plant cell walls to degradation [3–6].

Beyond the traditional monolignols, several other phenolic compounds, also derived from the phenylpropanoid pathway, have been shown to act as lignin monomers. These include monolignol ester conjugates, phenolic compounds from the truncated biosynthesis of monolignols, and ferulate esters, among others [7–11]. Recent research has revealed that phenolic compounds from other biosynthetic pathways, such as the flavonoid and hydroxystilbene pathways, can also participate in radical coupling reactions with monolignols or lignin oligomers, thereby becoming part of the lignin structure and expanding the traditional definition of lignin [10–13]. The most important example is the flavone tricin that has been identified as a lignin monomer in grasses and other monocots [14–19]. In papyrus, additional flavonoids such as dihydrotricin, naringenin, and naringenin chalcone, along with tricin,

* Corresponding author at: Instituto de Recursos Naturales y Agrobiología de Sevilla (IRNAS), CSIC, Avda. Reina Mercedes, 10, 41012 Seville, Spain.
E-mail addresses: delrio@irnase.csic.es (J.C. del Río), jralph@wisc.edu (J. Ralph), benitez@icmse.csic.es (J.J. Benítez), susana.guzman@csic.es (S. Guzman-Puyol), ja.heredia@csic.es (J.A. Heredia-Guerrero), jrencoret@irnase.csic.es (J. Rencoret).

https://doi.org/10.1016/j.ijbiomac.2025.145570
Received 25 March 2025; Received in revised form 11 June 2025; Accepted 25 June 2025
Available online 26 June 2025

were also found incorporated into the lignin [20,21]. Similarly, hydroxystilbenes like resveratrol, isorhapontigenin, and piceatannol have been detected in the lignin of palm fruit endocarps [22,23], and their *O*-glucosylated counterparts, such as piceid, astringin, and isorhapontin, have been found in spruce bark lignin [24,25]. These findings not only broaden our understanding of lignin biosynthesis but also demonstrate that lignin is a highly dynamic and adaptable polymer, capable of incorporating a diverse array of phenolic compounds across different species and tissues [10–12].

Ferulic acid amides represent another significant group of phenolic compounds that have been reported to be incorporated into the plant cell walls, particularly within the Solanaceae family. Feruloyltyramine and feruloyloctopamine, for instance, have been shown to covalently bind to the cell walls of both natural and wound periderms in potato (*Solanum tuberosum*) tubers [26]. Feruloyltyramine has also been detected in the cell walls of other Solanaceae members, including tobacco (*Nicotiana tabacum*) [27–29], the related *Nicotiana attenuata* [30,31], and tomato (*Solanum lycopersicum*) [32]. Diferuloylputrescine has been found incorporated into the lignin of maize (*Zea mays*) kernels [33].

The specific binding of ferulic acid amides to various cell wall polymers remains a subject of controversy. In suberized tissues such as potato periderms, it has been proposed that feruloyltyramine predominantly binds to suberin [34–36]; however, other authors did not rule out its potential association with lignin or other cell wall components [26]. These conflicting findings highlight the complexity of cell wall architecture and suggest that the binding behavior of feruloyltyramine may vary according to tissue type. Consequently, the precise modes of incorporation of ferulic acid amides within the cell walls of potato periderms remain unresolved, raising important questions about their role in cell wall reinforcement and their interactions with lignin, suberin, or other biopolymers.

To investigate the modes of incorporation of ferulic acid amides into the cell wall biopolymers of potato periderms, we isolated a lignin/suberin-enriched fraction from finely milled, extractive-free potato periderm samples using aqueous dioxane extraction. This fraction was then thoroughly analyzed using advanced analytical techniques such as Derivatization Followed by Reductive Cleavage (DFRC) to identify the lignin monomers involved in β-ether linkages, Gel-Permeation Chromatography (GPC) to determine the molecular weight distribution, and two-dimensional Nuclear Magnetic Resonance (2D-NMR) spectroscopy for detailed structural elucidation of the ferulic acid amides, and the various lignin units characterized by their inter-unit linkages. This study aims to clarify how these ferulic acid amides are integrated into the cell wall and provides new insights into the biochemical pathways involved in the lignification/suberization of potato periderms.

2. Materials and methods

2.1. Plant material

Potato tubers (*Solanum tuberosum*, var. Agria), field-grown in Seville, Spain, were selected for the present study. The potato periderms were mechanically removed, thoroughly washed with water, and allowed to air dry. The dried periderms were milled in an IKA MF 10 knife mill (IKA, Staufen, Germany) to pass through a 1 mm screen. The milled periderm material was then subjected to sequential extraction in a Soxhlet apparatus to remove all extractives. The extraction process involved four solvents: dichloromethane (8 h), ethanol (18 h), water (24 h), and methanol (18 h), applied successively in this order to ensure complete removal of soluble compounds of different polarity. The yield of the extractive-free potato periderms represented 86.1% ± 4.9% of the original material mass.

2.2. Isolation and purification of a lignin/suberin-enriched fraction

The lignin/suberin-enriched fraction was isolated from extractive-free potato periderms using dioxane–water extraction. Initially, around 100 g of pre-extracted potato periderms were ball milled in a Retsch PM-100 planetary mill (Retsch, Haan, Germany), using a 500 mL agate jar with 20 × 20 mm agate bearings at 400 rpm for 5 h, creating a fine powder. This powder was then extracted with a 96:4 (*v*/v) dioxane: water mixture for 16 h to solubilize the lignin/suberin fraction, which was separated by centrifugation. This extraction was repeated twice with fresh dioxane:water solution. The combined extracts were evaporated to dryness under reduced pressure at 40 °C using a rotary evaporator. Finally, the crude extract was purified as described elsewhere [37]. Briefly, the residue was redissolved in acetic acid:water 9:1 (v/v), then precipitated into water. The resulting solid was collected by centrifugation, ground in an agate mortar, and dissolved in 1,2-dichloroethane:ethanol (2:1, v/v). After centrifugation to remove insoluble material, the supernatant was precipitated into diethyl ether. The recovered residue was washed with petroleum ether via centrifugation, yielding a purified lignin/suberin fraction that was dried under a nitrogen stream. The yield of the lignin/suberin fraction accounted for around 5% of the pre-extracted potato periderms.

2.3. Derivatization followed by reductive cleavage (DFRC)

DFRC was carried out using the experimental conditions previously described [37,38]. Briefly, approximately 5 mg of the lignin/suberin-enriched fraction was reacted with acetyl bromide in acetic acid (8:92, v/v) for 2 h at 50 °C, followed by treatment with Zn powder (50 mg) for 40 min at room temperature. The DFRC degradation products were then acetylated for 2 h in 1.1 mL of dichloromethane containing 0.2 mL of acetic anhydride and 0.2 mL of pyridine for subsequent GC/MS analysis. The analysis was carried out on a Shimadzu GC/MS-QP2020 instrument (Shimadzu Co., Kyoto, Japan) equipped with a DB-5MS capillary column (30 m × 0.25 mm I.D., 0.25 μm film thickness) from J&W Scientific (Folsom, CA). The oven temperature program was as follows: 140 °C (1 min hold), ramped at 3 °C min^{-1} to 250 °C, then at 3 °C min^{-1} to 280 °C (1 min hold), and finally at 20 °C min^{-1} to 300 °C (18 min hold). The injector and transfer line temperatures were maintained at 250 °C and 310 °C, respectively, with helium carrier gas at a flow rate of 1 mL min^{-1}. Standards of feruloyltyramine and feruloyloctopamine were purchased from Sigma-Aldrich, and were also subjected to DFRC degradation using the same conditions.

2.4. Two-dimensional nuclear magnetic resonance (2D-NMR) spectroscopy

2D-NMR spectra (HSQC, HMBC, HSQC-TOCSY) experiments were acquired on an AVANCE III 500 MHz instrument (Bruker, Karlsruhe, Germany) equipped with a 5 mm TCI (triple resonance; ^{1}H, ^{13}C, ^{15}N) gradient cryoprobe with inverse geometry (proton coils closest to the sample). Approximately 60 mg of lignin/suberin enriched sample were dissolved in 0.6 mL of DMSO-d_6. The HSQC experiments used Bruker's standard "hsqcetgpsisp2.2" pulse program (adiabatic-pulsed version). The HMBC experiments used the "hmbcgplpndqf" pulse program with long-range *J*-coupling evolution times of 62.5 ms (J_{LR} = 8 Hz) or 80 ms (J_{LR} = 6.25 Hz). The HSQC-TOCSY experiments used the "hsqcdietgpsisp.2" pulse program with a TOCSY mixing time of 80 ms. The central solvent peaks were used as internal references (δ_C/δ_H 39.5/2.49). The detailed experimental conditions have been described elsewhere [37]. A semi-quantitative analysis was performed by integrating the HSQC cross-signal volumes using Bruker's Topspin 3.5. In the aliphatic oxygenated region, the relative abundances of the various inter-unit linkages were determined from the C_α/H_α correlations (signals $\mathbf{A}_\alpha$, $\mathbf{B}_\alpha$, $\mathbf{C}_\alpha$) and the equivalent C_7/H_7 correlations (signal $\mathbf{B_{Ft7}}/\mathbf{B_{Fo7}}$). For the quantification of the relative abundances of the lignin aromatic units,

the signals $S_{2,6}$, G_2, $H_{2,6}$ in the aromatic region were used; as signals $S_{2,6}$ and $H_{2,6}$ involve two proton-carbon pairs, their volume integrals were halved.

2.5. Gel-permeation chromatography (GPC)

The lignin/suberin fraction was initially acetylated using a mixture of acetic anhydride and pyridine (1:1, v/v) and then dissolved in tetrahydrofuran (THF) for GPC analysis. The GPC system employed was a Shimadzu Prominence-I LC-2030 3D (Shimadzu, Kyoto, Japan), equipped with a 300 mm × 7.5 mm i.d., 5 μm, PLgel MIXED-D column (Agilent Technologies, Stockport, United Kingdom) and a photodiode array (PDA) detector using 280 nm wavelength. The eluent, THF, was maintained at 40 °C with a flow rate of 0.5 mL min^{-1}. Data acquisition and processing were performed using LabSolution GPC software (version 5.82, Shimadzu, Kyoto, Japan). A calibration curve was constructed using a polystyrene standards kit (Agilent Technologies, Stockport, United Kingdom) with a molecular mass (Mr) range of 5.8 × 10^2 to 3.24 × 10^6 Da.

3. Results and discussion

3.1. Release of ferulic acid amides from the lignin/suberin-enriched fraction of potato periderms by chemical cleavage of the alkyl-aryl ether linkages

The lignin/suberin-enriched fraction isolated from potato periderms was first analyzed using Derivatization Followed by Reductive Cleavage (DFRC), a chemical degradation method similar to thioacidolysis that selectively cleaves β-ether linkages in lignin but releases the corresponding lignin monomers from these non-condensed units by a distinctly different mechanism [38]. The chromatogram of the lignin monomers released from the lignin/suberin-enriched fraction by DFRC is shown in Fig. 1. The released lignin monomers included the *cis*- and *trans*-isomers of the *p*-hydroxyphenyl (*t***H**), guaiacyl (*c***G**, and *t***G**), and syringyl (*c***S**, and *t***S**) monomers (as their acetylated derivatives), with

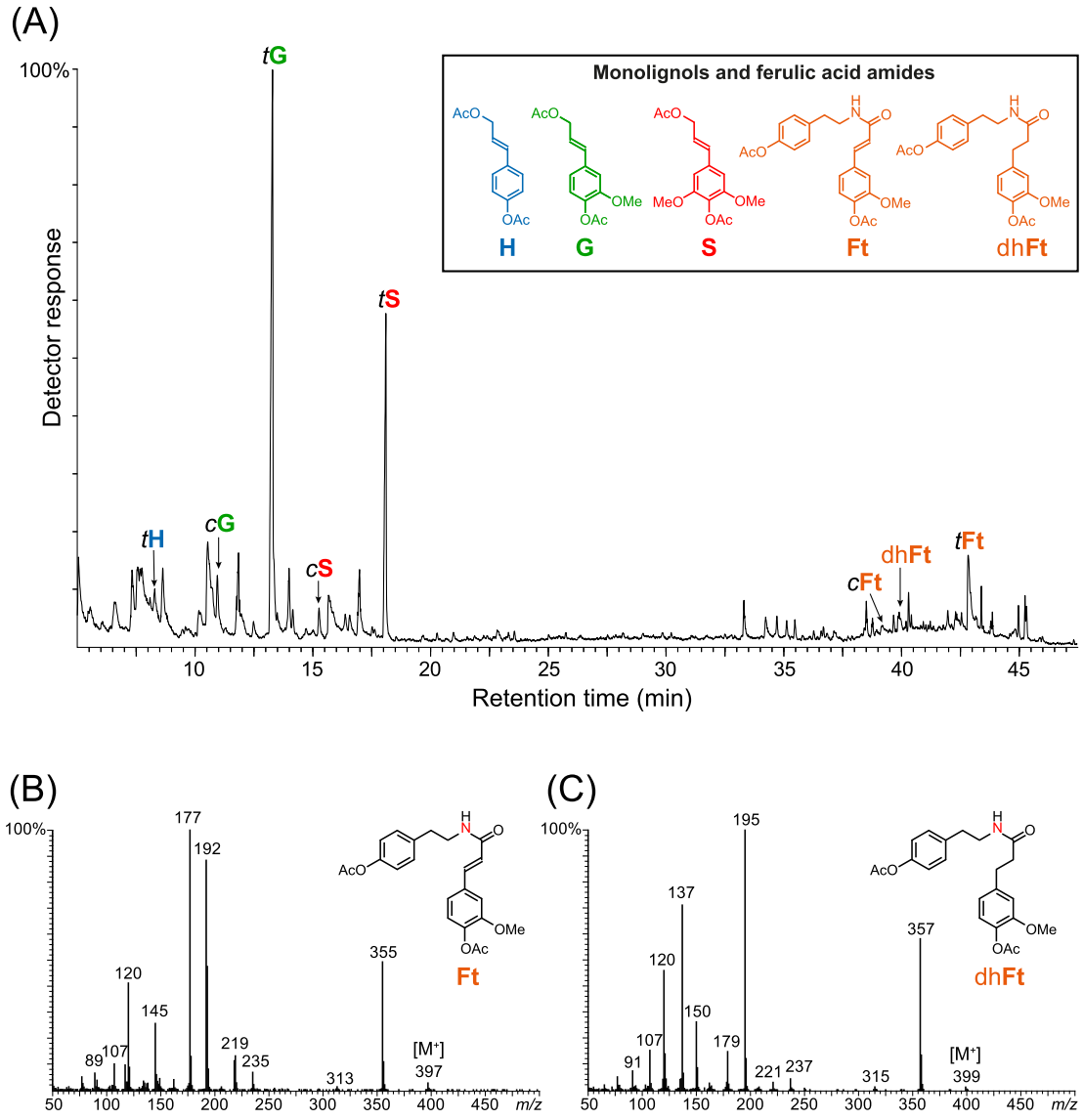

Fig. 1. (A) Chromatogram of the DFRC degradation products released from the lignin/suberin-enriched fraction of potato periderms. *t***H**, *c***G**, *t***G**, *c***S**, and *t***S** are the *cis*- and *trans*-*p*-hydroxyphenyl (**H**), coniferyl (**G**), and sinapyl (**S**) alcohol monomers (as their acetate derivatives). *c***Ft** and *t***Ft** are the *cis*- and *trans*-isomers of feruloyltyramine (as their acetate derivative), dh**Ft** is the dihydroferuloyltyramine (as its acetate derivative). The structures of the released compounds are indicated in the inset. (B) Electron-impact mass spectrum and structure of feruloyltyramine (acetylated). (C) Electron-impact mass spectrum and structure of dihydroferuloyltyramine, dh**Ft** (acetylated).

guaiacyl units predominating. An estimation of the lignin composition indicated an **H**:**G**:**S** ratio of 2:69:29 (**S**/**G** ratio of 0.42). A similar composition was obtained through thioacidolysis on the lignin-domain of suberized tissues of potato periderms [39]. But most interestingly, significant amounts of the *cis*-, and *trans*-isomers of feruloyltyramine (*c***Ft**, and *t***Ft**) (as their acetylated derivatives) were also released. Amides remain intact during DFRC, as previously noted for the corresponding esters, a distinctly useful aspect of the DFRC method – the ability to cleave ethers while retaining the key ester (and amide) conjugates [40–43]. The identity of feruloyltyramine was confirmed by comparison with the retention time and mass spectrum of an authentic standard (Fig. 1B). Feruloyltyramine, along with minor amounts of feruloyloctopamine (see structure of feruloyloctopamine, Fo, in Fig. 2), was also released by thioacidolysis from natural and wounded potato periderms [26], indicating that they were bound to the cell wall through β-ether bonds. However, although no traces of feruloyloctopamine could be detected in the DFRC analysis, small amounts of a compound that was identified as dihydroferuloyltyramine (dh**Ft**) were unexpectedly released (Fig. 1C).

The unexpected release of dh**Ft** instead of the anticipated feruloyloctopamine prompted us to study the behavior of authentic standards of ferulic acid amides upon DFRC degradation. Surprisingly, both feruloyltyramine and feruloyloctopamine yielded predominantly dh**Ft** upon DFRC, along with minor amounts of feruloyltyramine. This result suggested that during DFRC the unsaturated bond in the ferulate moiety becomes saturated, while the hydroxyl group on the octopamine side-chain was eliminated thus precluding the detection of feruloyloctopamine. Intriguingly, however, feruloyltyramine was also readily released from the lignin/suberin-enriched fraction with its double-bond intact, implying that both feruloyltyramine and its unsaturated counterpart dh**Ft** may derive from the same feruloyltyramine and feruloyloctopamine units, differing only in the type of ether linkage present. It was reported that both feruloyltyramine and feruloyloctopamine are bound to the cell wall through 4−*O*- and 8−*O*-ether bonds [26], which are prone to DFRC cleavage, and these distinct linkages appear to influence their behavior under DFRC conditions, as indicated in Fig. 2. Hence, when feruloyltyramine is linked through 4−*O*- ether linkages DFRC converts it into dh**Ft**, similarly to the conversion of monolignol *p*-coumarates into their saturated counterparts [43]. In the case of feruloyloctopamine linked via 4−*O*-ether bond, the double bond in the ferulate moiety is similarly reduced whereas the 7′-OH group undergoes bromination in the first acetyl bromide step of DFRC and subsequent reduction in the second step, also resulting in the formation of dh**Ft**. In contrast, when the linkage occurs through 8−*O*-ether bonds,

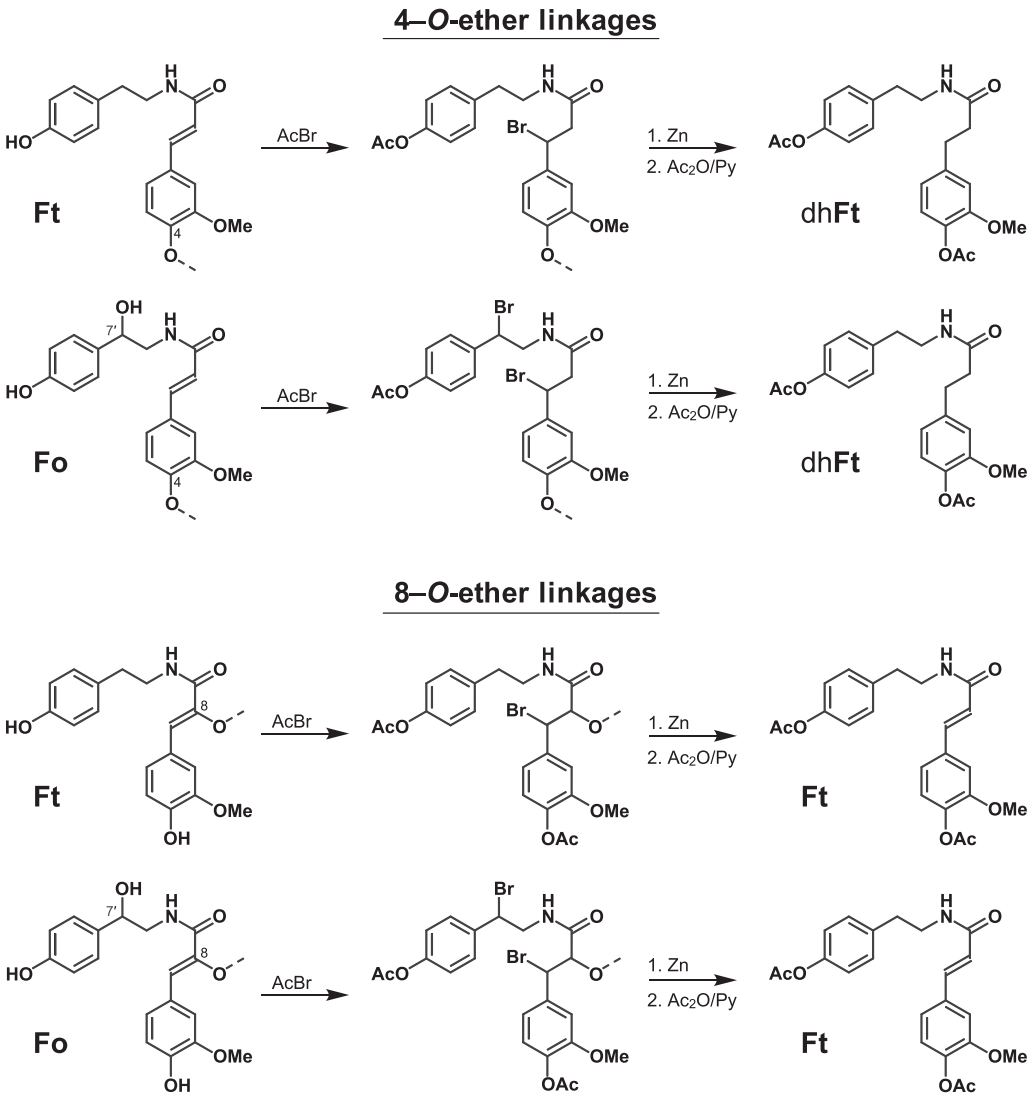

Fig. 2. Pathway of the DFRC degradation of the ferulic acid amides linked through 4−*O*- vs 8−*O*- ether bonds. **Ft**: feruloyltyramine; **Fo**: feruloyloctopamine; dh**Ft**: dihydroferuloyltyramine.

the reductive elimination of the substituent at the 8-position results in retention of the double-bond during DFRC, as shown in Fig. 2. In other words, in the case of feruloyltyramine, bromination at the 7-position followed by elimination of both the bromide and the 8-substituent preserves the double bond; similarly, feruloyloctopamine retains the double bond while the 7′-OH is brominated and subsequently reduced, ultimately forming feruloyltyramine.

The amounts of feruloyltyramine released after DFRC of the lignin/suberin-enriched fraction of potato periderms, which predominantly derive from the ferulic acid amides linked through 8−*O*-ether bonds, accounted for around 15% of the total released lignin units (H+G+S=100), whereas the amounts of dh**Ft**, which derived from ferulic acid amides linked through 4−*O*-ether bonds, accounted for about 4%. The release of significant amounts of feruloyltyramine and dh**Ft** indicates that feruloyltyramine (and likely also feruloyloctopamine) are incorporated into the cell wall polymers of potato periderms and that at least a part of it is attached through β-ether linkages, the ones cleaved by DFRC. Moreover, the data also indicate that the ferulic acid amides are linked through both 4−*O*- and 8−*O*-ether linkages, with the latter being more prevalent. These ferulic acid amides, however, would be expected to couple and cross-couple with other ferulic acid amides or with lignin units through different types of linkages, including condensed linkages that are not amenable to DFRC degradation. As the DFRC degradation method only cleaves ether bonds, the amounts of feruloyltyramine (and feruloyloctopamine) released therefore only corresponded to those units linked through ether bonds, and the actual amounts of feruloyltyramine incorporated into the lignin of potato periderms would likely be much higher than the amounts we are able to release by DFRC. Additional information regarding the different modes of incorporation of feruloyltyramine and feruloyloctopamine into the lignin of potato periderms was obtained by detailed NMR analyses described below.

3.2. Identification of ferulic acid amides incorporated into the lignin/suberin-enriched fraction of potato periderms by 2D-NMR spectroscopy

The lignin/suberin-enriched fraction isolated from potato periderms was also analyzed using 2D-NMR HSQC, HSQC-TOCSY, and HMBC experiments of the sample in DMSO-d_6 to obtain additional insights into the distribution of aromatic units and inter-unit linkages. The HSQC spectrum is depicted in Fig. 3. For clarity, the HSQC spectrum was divided into three distinct regions, aliphatic (δ_C/δ_H 30–50/1.5–4.0), oxygenated-aliphatic (δ_C/δ_H 50–90/2.8–6.0), and aromatic (δ_C/δ_H 100–142/6.0–8.0). The identified lignin structural units, ferulic acid amides, and lignin units with their characteristic inter-unit linkages are also shown in Fig. 3. The most relevant structural characteristics of the lignin/suberin-enriched fraction are shown in appropriate boxes in Fig. 3, including the relative abundances of the different lignin units (**H**, **G**, and **S**), the relative contents of ferulic acid amides, and lignin structural units **A**-**C**, estimated from the volume-integration of the signals in the HSQC spectrum.

The aromatic region of the HSQC spectrum (Fig. 3C) provided insights into the different aromatic units present in the lignin/suberin preparation. Characteristic signals corresponding to S- and G-lignin units were clearly identified, alongside a minor signal from H-lignin units. The estimation of the lignin composition indicated a predominance of G-lignin units, with an **H**:**G**:**S** ratio of 2:70:28 (**S**/**G** ratio of 0.40), similar to that found by DFRC. The oxygenated-aliphatic region of the spectrum (Fig. 3B) provided detailed insights into the various inter-unit linkages present in the lignin. In this region, distinct signals corresponding to typical lignin substructures were observed, including β−*O*−4′ alkyl-aryl ethers **A** (73% of all linkages identified), β−5′ phenylcoumarans **B** (9%), and β−β′ resinols **C** (4%). Despite the enrichment in G-lignin units observed in this lignin, dibenzodioxocin structures, which are formed via 5–5-coupling of lignin oligomers followed by 4–*O*–β-coupling with a monolignol and are usually abundant in G-rich lignins [44], could only be barely detected.

The HSQC spectrum also revealed a series of signals that were unambiguously assigned to the ferulic acid amides feruloyltyramine **Ft** and feruloyloctopamine **Fo**, further corroborating the structural assignments previously established by DFRC, and providing direct evidence for the presence of feruloyloctopamine that had only been inferred indirectly from the DFRC analysis. The aromatic region of the HSQC spectrum (Fig. 3C) presented the characteristic signals for the C_7/H_7 and C_8/H_8 correlations of the unsaturated moieties of the ferulic acid amides at δ_C/δ_H 138.6/7.30 (**Ft**$_7$/**Fo**$_7$), and at δ_C/δ_H 118.9/6.41 (**Ft**$_8$/**Fo**$_8$). These signals are diagnostic for ferulic acid amides and are similar to those of the diferuloylputrescine found incorporated into the lignin in maize kernels [33]. This region of the spectrum also contains signals corresponding to the remaining C_2/H_2 and C_6/H_6 correlations of the ferulate moieties at δ_C/δ_H 110.5/7.11 (**Ft**$_2$/**Fo**$_2$) and at δ_C/δ_H 120.8/6.98 (**Ft**$_6$/**Fo**$_6$), and the C_5/H_5 correlations at around δ_C/δ_H 115.3/6.76, overlapped with other signals, that are also typical of ferulic acid amides [33]. The correlation signals for the tyramine and octopamine moieties attached to the feruloyl amide were also readily observed in the spectrum. Thus, the aromatic region of the HSQC spectrum (Fig. 3C) shows the typical signals for the $C_{2',6'}/H_{2',6'}$ correlations for tyramine at δ_C/δ_H 129.3/6.90 (**Ft**$_{2',6'}$), and for octopamine at δ_C/δ_H 126.8/7.13 (**Fo**$_{2',6'}$). In addition, the correlation signals of the aliphatic sidechains of the tyramine and octopamine moieties were readily observed in the aliphatic and the oxygenated-aliphatic regions of the HSQC spectrum. Thus, the signals for the $C_{7'}/H_{7'}$ and $C_{8'}/H_{8'}$ correlations of tyramine were observed in the aliphatic part of the spectrum (Fig. 3A) at δ_C/δ_H 34.0/2.63 (**Ft**$_{7'}$) and at δ_C/δ_H 40.4/3.32 (**Ft**$_{8'}$), respectively. Likewise, the double signal for the $C_{8'}/H_{8'}$ correlation of octopamine was seen in the aliphatic region of the spectrum at δ_C/δ_H 46.8/3.17 and 3.36 (**Fo**$_{8'}$), whereas the signal for $C_{7'}/H_{7'}$ that bears a hydroxyl group was seen in the oxygenated-aliphatic part of the spectrum (Fig. 3B) at δ_C/δ_H 70.9/4.54 (**Fo**$_{7'}$). All these signals conclusively demonstrate the occurrence of feruloyltyramine and feruloyloctopamine in the lignin/suberin-enriched fraction of potato periderms. To verify these assignments, the HSQC spectrum of this fraction was compared with the HSQC spectra of authentic standards of feruloyltyramine and feruloyloctopamine (Fig. 4). The near-exact match between the NMR signals confirmed the presence of these two ferulic acid amides in the lignin/suberin-enriched fraction of potato periderms. They are nevertheless present not as the simple conjugates but in the polymeric material as evidenced below.

The definitive assignments of these structures were also confirmed through HSQC-TOCSY and HMBC experiments that clearly demonstrated that the tyramine and octopamine moieties were linked to the ferulate moieties through amide linkages, as seen in Fig. 5. The HSQC-TOCSY spectrum (Fig. 5A) provided correlations between the C7′ and C8′ carbons of the tyramine (δ_C 34.0 and 40.4), and octopamine sidechains (δ_C 70.9 and 46.8) with the sidechain protons within the same spin system, including the amide N−H, as well as the 7′-OH of octopamine (**Fo**$_{7'\text{-OH}}$); N−H and O−H signals are routinely seen in DMSO because it is a solvent that limits proton exchange [45]. The HSQC-TOCSY spectrum confirmed the presence of two distinct sidechains for tyramine and octopamine moieties. The HMBC experiment of Fig. 5B provided additional information regarding the long-range correlations of the C7′ and C8′ carbons in the sidechains between them and with the N−H that confirmed the tyramine and octopamine moieties. The HSQC-TOCSY and the HMBC spectra revealed a subtle but distinct chemical shift for the N−H of tyramine (at δ_H 8.01) compared to that of octopamine (at δ_H 7.95). Finally, Fig. 6 shows the region of the HMBC spectrum correlating the carbonyl carbons of the feruloyl amides at around δ_C 165.0 with all protons within three bonds, namely the N−H and the H8′ of the tyramine (**Ft**$_{8'}$) and octopamine (**Fo**$_{8'}$) moieties, and the unsaturated protons (H7 and H8) of the ferulate sidechain (**Ft**$_7$/**Fo**$_7$, and **Ft**$_8$/**Fo**$_8$). For clarity, Fig. 6B highlights the relevant regions of the HSQC spectrum at which the signals for the $C_{8'}/H_{8'}$ correlations of the tyramine (**Ft**$_{8'}$) and octopamine (**Fo**$_{8'}$) sidechains, as well as the C_7/H_7 and C_8/H_8

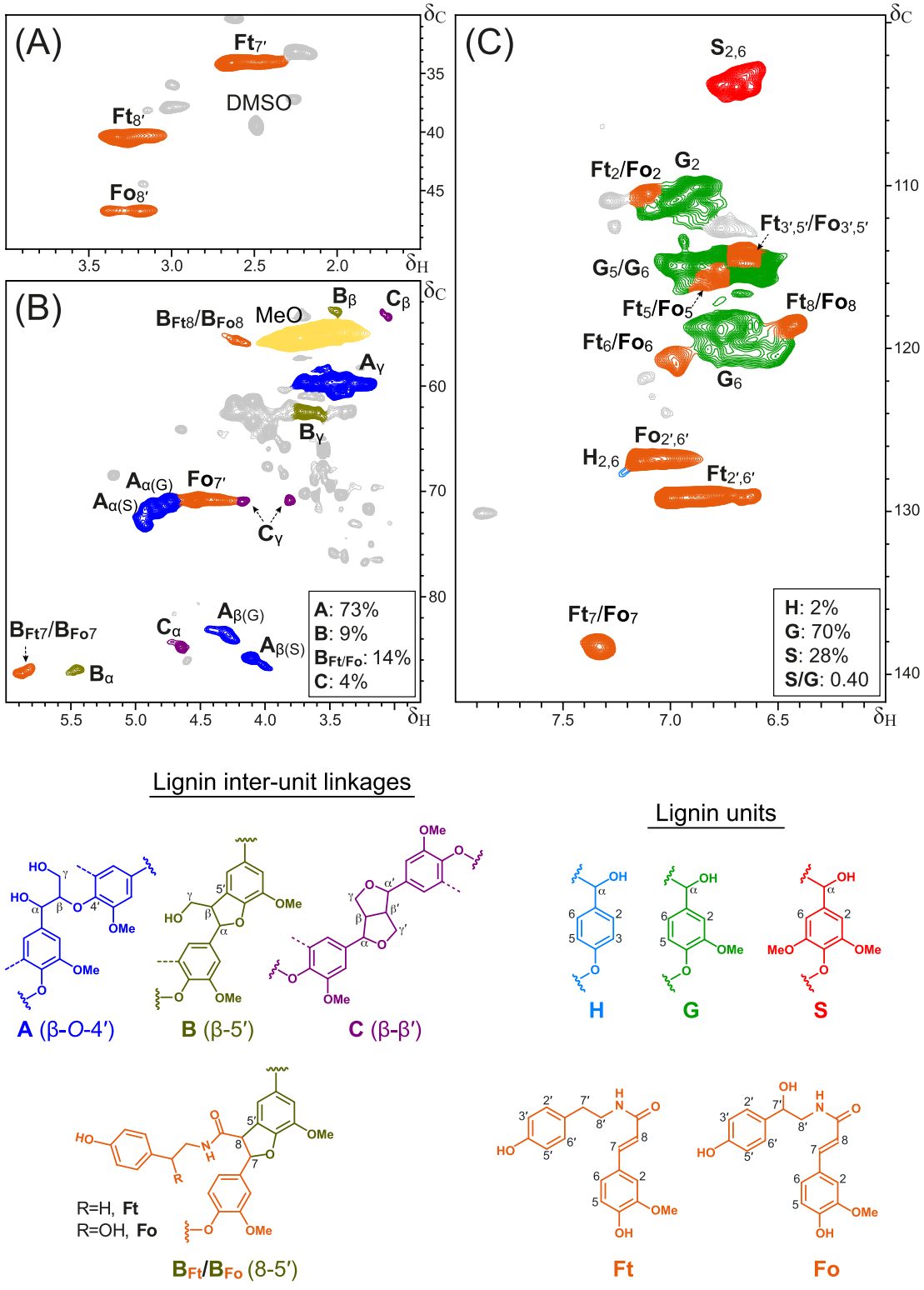

Fig. 3. 2D HSQC NMR spectrum (in DMSO-d_6) of the lignin/suberin-enriched fraction of potato periderms. (A) Aliphatic (δ_C/δ_H 30–50/1.5–4.0), (B) oxygenated-aliphatic (δ_C/δ_H 50–90/2.8–6.0), and (C) aromatic (δ_C/δ_H 100–142/6.0–8.0) regions. Main structures found are as follows: **A**, β–*O*–4′ alkyl-aryl ethers; **B**, β–5′ phenylcoumarans; $\mathbf{B_{Ft}/B_{Fo}}$, 8–5′ phenylcoumarans involving feruloyltyramine (**Ft**) and feruloyloctopamine (**Fo**); **C**, β–β′ resinols; **H**, *p*-hydroxyphenyl units; **G**, guaiacyl units; **S**, syringyl units; **Ft**, feruloyltyramine; **Fo**, feruloyloctopamine. The percentages for the various lignin inter-unit linkages (**A**, **B**, $\mathbf{B_{Ft}/B_{Fo}}$, **C**) were estimated from volume-integration and total 100 %. The percentages for the various lignin units (**H**, **S**, **G**) were also estimated from volume-integration.

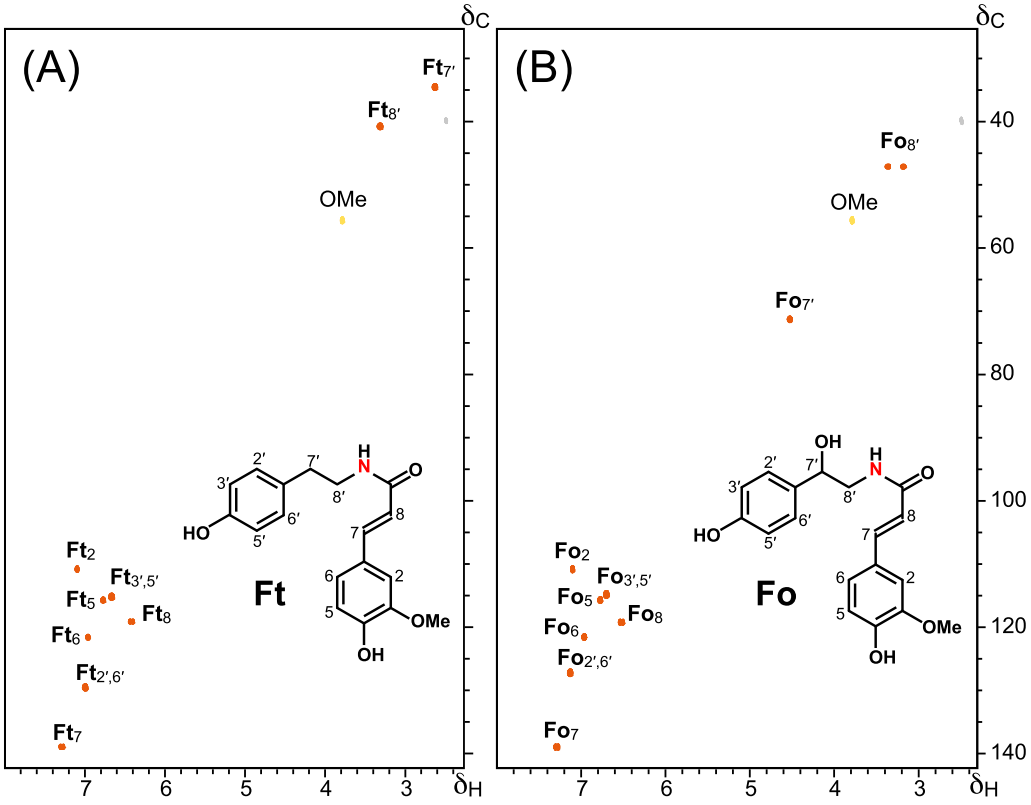

Fig. 4. 2D HSQC NMR spectra in DMSO-d_6 (δ_C/δ_H 25–142/2.3–8.0) of authentic standards of (A) feruloyltyramine **Ft**; (B) feruloyloctopamine **Fo**.

correlations of the feruloyl units, are observed. All these correlations are diagnostic for the occurrence of feruloyltyramine (**Ft**) and feruloyloctopamine (**Fo**) in the lignin/suberin-enriched fraction of potato periderms. However, it is important to note that, as all protons from the ferulates, particularly those from the C7 and C8 unsaturated moieties, are clearly observed in the spectra, these signals correspond exclusively to the feruloyltyramine and feruloyloctopamine structures that are present as end-groups with the double bond intact and not those that are expected to be coupled at their 4−*O*-, 5-, or 8-positions.

3.3. Modes of incorporation of feruloyltyramine and feruloyloctopamine into the cell wall polymers of potato periderms

Ferulic acid amides are good substrates of peroxidases in vitro [27]. As with other ferulate conjugates, the ferulate moiety in feruloyltyramine and feruloyloctopamine can be oxidized by peroxidases and/or laccases, forming radicals stabilized by resonance (Fig. 7). These radicals can then participate in radical coupling reactions with other ferulates, monolignols, or the growing lignin polymer at their 4−*O*-, 5-, and 8-positions, ultimately incorporating into the cell wall. In principle, the phenolic group of the tyramine and octopamine moieties can also undergo oxidation, forming radicals delocalized over their aromatic rings, providing additional sites for radical coupling at the 4′−*O*- and 3′-positions (Fig. 7). The different modes of incorporation of feruloyltyramine and feruloyloctopamine into the cell wall through 8-, 4−*O*-, and 4′−*O*-ether linkages, as well as through 8–5′-linkages forming phenylcoumaran structures, are also depicted in Fig. 7B. Although coupling at the 3′/5′ positions is theoretically possible for tyramine and octopamine units, no such products have been observed. Furthermore, although coupling at the 4′−*O* position has been previously reported [26], our findings suggest that the extent of these coupling products may have been overestimated, as demonstrated in the following sections.

The presence of strong correlation signals for C_7/H_7 at δ_C/δ_H 87.3/5.88 ($\mathbf{B_{Ft7}}$ and $\mathbf{B_{Fo7}}$) and C_8/H_8 at δ_C/δ_H 55.6/4.21 ($\mathbf{B_{Ft8}}$ and $\mathbf{B_{Fo8}}$) in the oxygenated-aliphatic region of the HSQC spectrum (Fig. 3B), assigned to 8–5′ phenylcoumaran structures involving feruloyltyramine ($\mathbf{B_{Ft}}$) and feruloyloctopamine ($\mathbf{B_{Fo}}$), strongly supports the participation of ferulic acid amides in radical coupling reactions. These signals closely resemble those previously reported for other ferulic acid amides involved in 8–5′ linkages forming phenylcoumaran structures [33], as well as for ferulates in similar structures [46,47], and clearly indicates that feruloyltyramine and feruloyloctopamine are incorporated into the cell wall polymers of potato periderms through 8–5′ linkages forming such phenylcoumaran structures. The definitive assignments of these signals were achieved through long-range correlation experiments in the HMBC spectrum (Fig. 8A) that clearly demonstrated that they correspond to phenylcoumaran structures involving the ferulate moieties of both feruloyltyramine and feruloyloctopamine. The HMBC spectrum shows that the carbonyl carbon (C9) of the feruloyl amide in these phenylcoumaran structures (at δ_C 169.2) correlates with the characteristic N−H proton of phenylcoumarans involving ferulic acid amides at δ_H 8.35 [33], as well as with the H7 (at δ_H 5.88) and H8 protons (at δ_H 4.21) of the phenylcoumaran structures. Additionally, the carbonyl carbon correlates with the H8′ of the tyramine ($\mathbf{Ft_{H8'}}$) and octopamine ($\mathbf{Fo_{H8'}}$) sidechains confirming their participation in this coupled structure. Further evidence for the involvement of feruloyltyramine in the phenylcoumaran structure comes from the correlation between the characteristic N−H proton and the C8′ carbon of tyramine ($\mathbf{Ft_{C8'}}$) at δ_C 40.7. The expected correlation between the N−H proton and the C8′ carbon of feruloyloctopamine ($\mathbf{Fo_{C8'}}$), which should appear at δ_C 46.8 (see dashed circle in Fig. 8A), however, was barely detected and appears only as a weak signal. Other correlation signals supporting the occurrence of these coupled phenylcoumaran structures are also shown in the HMBC spectrum in Fig. 8A. Additional correlations, such as those between C3′,5′ and the C2′,6′ positions of the aromatic rings of the tyramine and octopamine moieties, or the correlations with the C5″ of the second (guaiacyl or ferulate) unit, are clearly observed but not detailed in the figure for clarity.

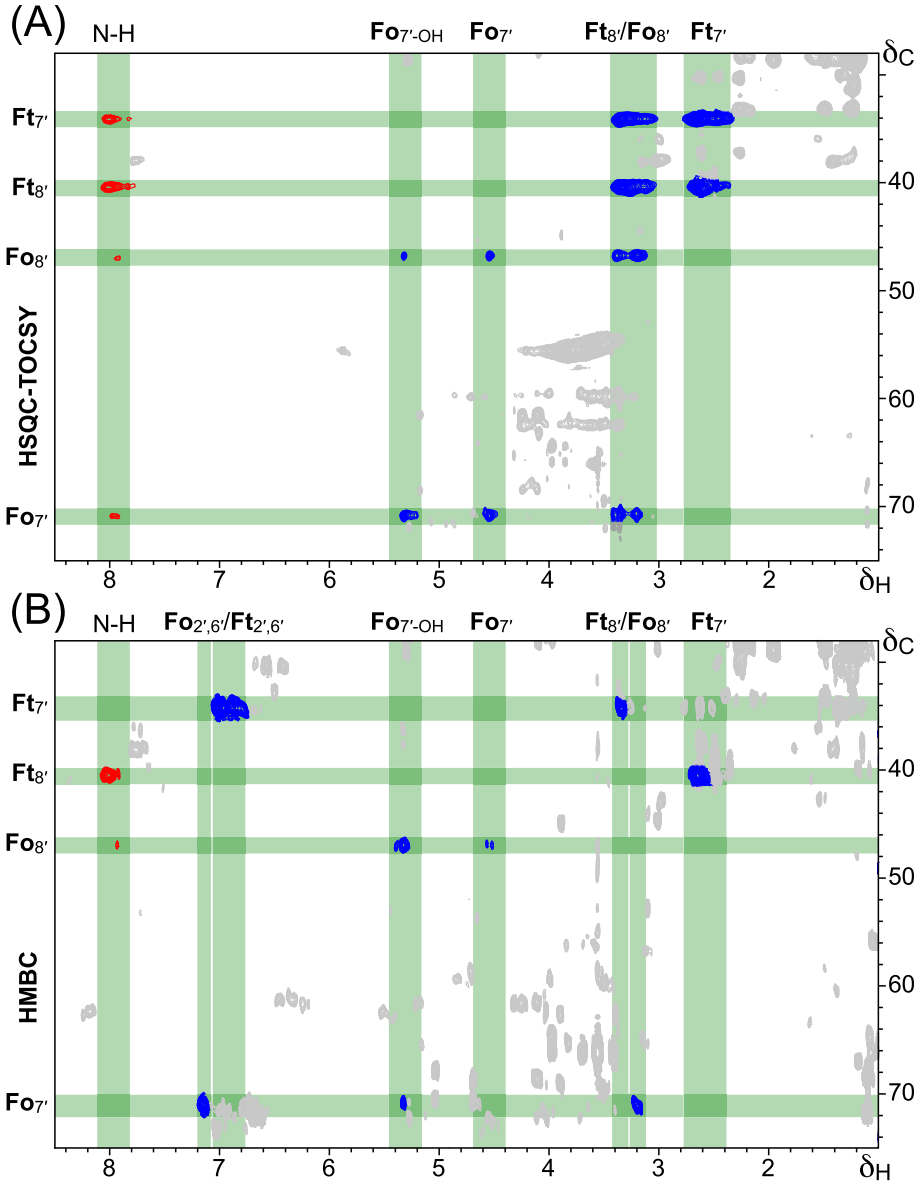

Fig. 5. (A) Partial HSQC-TOCSY spectrum (δ_C/δ_H 28–75/1.0–8.5) of the lignin/suberin-enriched fraction of potato periderms showing the main correlations for the aliphatic sidechains (C7′ and C8′) and the N−H of feruloyltyramine **Ft** and feruloyloctopamine **Fo** units. (B) Section of the HMBC spectrum (δ_C/δ_H 28–75/1.0–8.5) showing the main correlations for the aliphatic sidechains and the N−H of the feruloyltyramine and feruloyloctopamine units in the polymer. Signals colored red correspond to correlations with the N−H proton of the amide.

As noted above, although the HMBC signal indicating the involvement of feruloyltyramine in phenylcoumaran structures was clearly observed, the signal indicating the involvement of feruloyloctopamine in such phenylcoumaran structures was only barely detected. However, the participation of both feruloyltyramine and feruloyloctopamine in these phenylcoumaran structures was more clearly evidenced in the HSQC-TOCSY spectrum shown in Fig. 8B. The HSQC-TOCSY spectrum shows correlations between the C7′ and C8′ carbons of the tyramine and octopamine sidechains in phenylcoumaran structures and the sidechain protons within the same spin system, including the amide N−H. Although similar to the spectrum shown in Fig. 5A, here we have specifically highlighted the distinctive N−H correlation signal at δ_H 8.35 characteristic for phenylcoumaran structures involving ferulic acid amides, and which is clearly observed correlating with the C7′ and C8′ of feruloyltyramine and feruloyloctopamine. Although the N−H correlations with the C7′ and C8′ of feruloyloctopamine appear at lower intensities than those of feruloyltyramine, they still provide clear evidence for the involvement of both feruloyltyramine and feruloyloctopamine in phenylcoumaran structures.

The presence of these coupled phenylcoumaran structures provides compelling evidence for the participation of both feruloyltyramine and feruloyloctopamine in radical coupling reactions with other ferulic acid amides or with lignin G-units, to be integrally incorporated and covalently linked to the cell wall. The occurrence of other coupled structures involving feruloyltyramine and feruloyloctopamine, probably forming 5–5′, 8−*O*−4′, and other linkages, is also demonstrated by the existence of other signals for ferulic acid amides in the HMBC spectrum of Fig. 9. Signals colored red in the spectrum correspond to the N−H correlations of the amide and are diagnostic for feruloyltyramine and feruloyloctopamine. Different correlations for the carbonyl carbon (C9) of the amide group that corresponded to different linkages involving feruloyltyramine and feruloyloctopamine were apparent. Besides the 4−*O*, end-groups, and 8–5′ phenylcoumaran structures that have already been assigned, signals for other structures were apparent in the HMBC

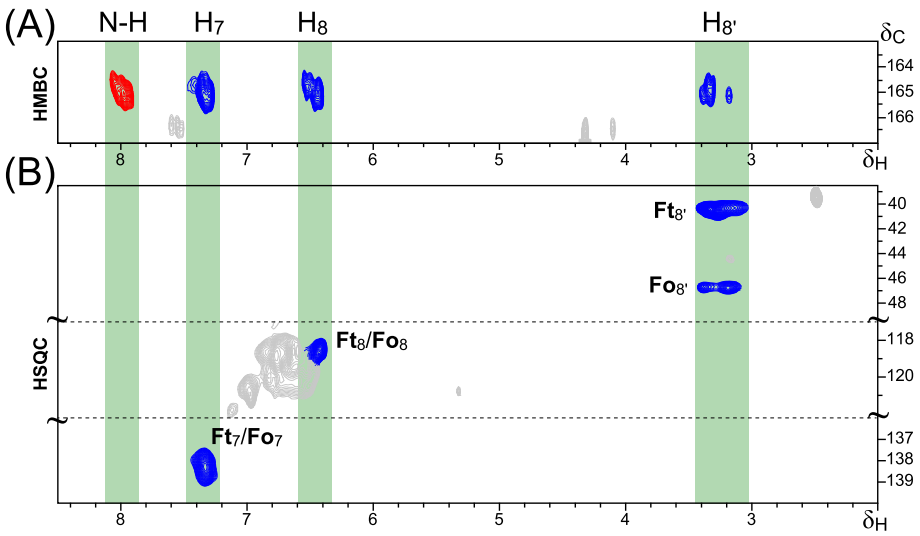

Fig. 6. (A) Section of the HMBC spectrum (δ_C/δ_H 162–167/2.0–8.5) of the lignin/suberin-enriched fraction of potato periderms showing the main correlations for the carbonyl carbons of feruloyltyramine **Ft** and feruloyloctopamine **Fo** units at δ_C 165.0. (B) Appropriate sections of the HSQC spectrum showing the $C_{8'}/H_{8'}$ correlations of the tyramine and octopamine moieties (δ_C 38–50) and the C_7/H_7 and C_8/H_8 correlations of the feruloyl units (δ_C 136–140 and 117–122, respectively). Signals colored red correspond to correlations with the N−H proton of the amide.

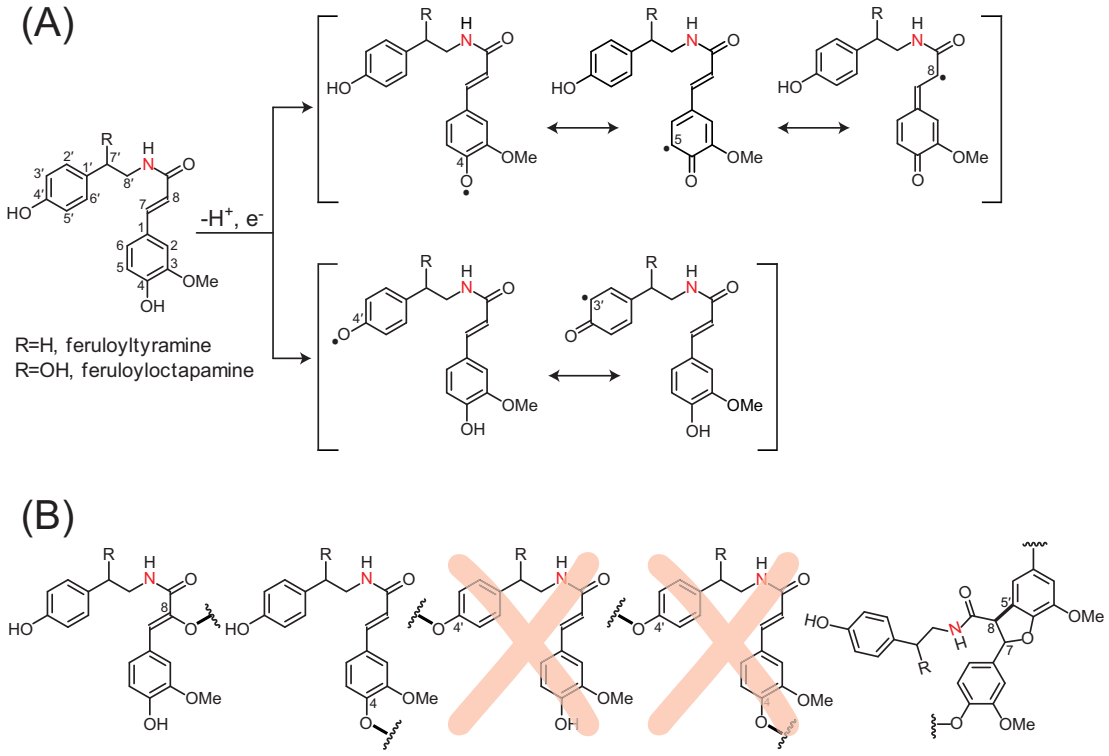

Fig. 7. (A) Oxidative radicalization of feruloyltyramine and feruloyloctopamine showing resonance forms with electron density at the 4–*O*-, 5-, and 8-positions of the ferulate moiety. In principle, the tyramine and octopamine moieties may also be oxidized in the same manner producing a radical that is stabilized by resonance and can couple at its 4′–*O*-, and 3′- positions. (B) Different modes of incorporation of feruloyltyramine into the cell walls through 8-, 4–*O*-, and 4′–*O*- ether linkages and through 8–5′ linkages forming phenylcoumaran structures. In principle, tyramine and octopamine units can react at 3′/5′ as well but the products have not been identified to date. Although coupling structures at the 4′-OH position have been previously reported, the present work shows that they do not contribute to the formation of ether linkages within the cell wall.

spectrum (Fig. 9). Hence, signals for 8−*O*−4′-coupled structures involving feruloyltyramine and feruloyloctopamine were tentatively assigned by comparison with the relative shifts of the carbonyl groups in the HMBC spectrum of similar 8−*O*−4′-coupled structures from other ferulic acid amides [33] and from ferulates [48,49]; the correlation signals for the carbonyl carbon in 8−*O*−4′-coupled structures appear upfield (at lower δ) in the spectrum and only show correlation with H7. These 8−*O*−4′ structures are responsible for the feruloyltyramine units released by DFRC and correspond to both feruloyltyramine and feruloyloctopamine units linked through 8−*O*−4′ ether linkages.

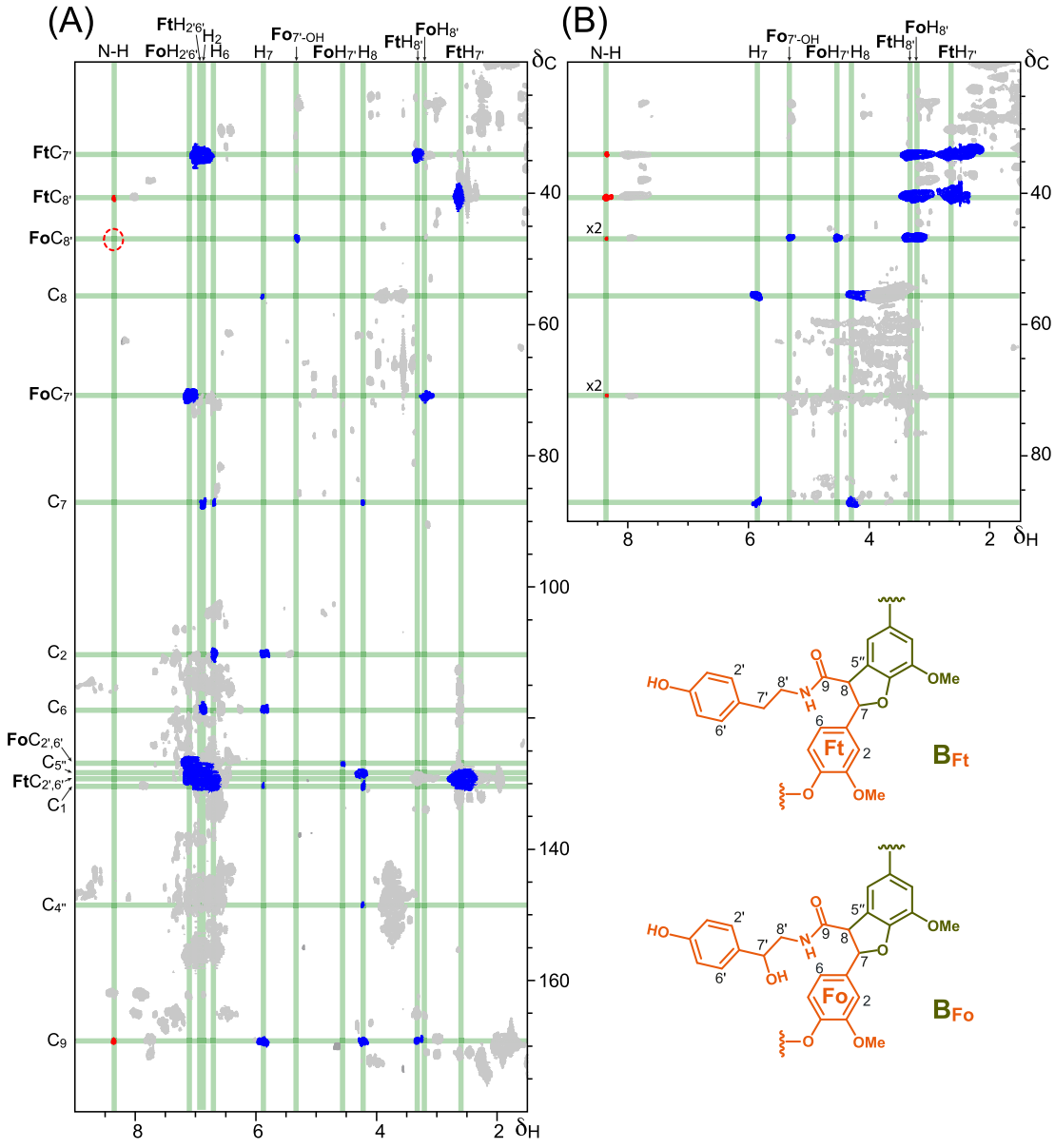

Fig. 8. Identification of 8–5 linkages involving **Ft** and **Fo**, leading to a phenylcoumaran structure. (A) HMBC spectrum (δ_C/δ_H 20–180/1.5–9.0) of the lignin/suberin-enriched fraction of potato periderms highlighting the key correlations for the 8–5″ phenylcoumaran structure involving feruloyltyramine ($\mathbf{B_{Ft}}$) and feruloyloctopamine ($\mathbf{B_{Fo}}$). (B) HSQC-TOCSY spectrum (δ_C/δ_H 20–90/1.5–9.0) showing the correlations between the C7′ and C8′ carbons of the tyramine and octopamine sidechains in phenylcoumaran structures and the sidechain protons within the same spin system, including the amide N–H. The correlations of the sidechains of feruloyltyramine and feruloyloctopamine (C7, C8) involved in the phenylcoumaran structures are also shown. Red-colored signals correspond to the N–H correlations from the amide group in the phenylcoumaran structures.

According to the NMR and DFRC data presented here, feruloyltyramine and feruloyloctopamine are covalently bound to the cell wall polymers of potato periderms through the ferulate moieties via 8–*O*–4-, and 4–*O*–β- ether linkages, as well as via 8–5 linkages forming phenylcoumaran structures. However, previous works indicated that a significant part of feruloyltyramine (up to 20% of all ether-linkages) was also attached to the cell wall through the phenolic group of the tyramine moiety [26]. These conclusions were drawn despite the limitations in the analytical methods used to determine the extent of etherification of the tyramine moiety. Given the issues with the determinations, it was suspected that the etherification level of the tyramine moiety was considerably lower, as already advanced [7,10]. In the present work, we provide evidence that demonstrate that the 4′-OH groups of both feruloyltyramine and feruloyloctopamine are largely unbound. Fig. 10A shows the region of the ^{1}H NMR spectrum of the lignin/suberin-enriched fraction of potato periderms where the characteristic signals corresponding to phenolic groups appear, whereas Fig. 10B shows the region of the HMBC spectrum displaying correlation signals between the phenolic groups of the ferulate moiety (4-OH) and the phenolic groups of the tyramine 4′-OH-(**Ft**), and octopamine 4′-OH-(**Fo**) moieties, that demonstrate the origin of the phenolic groups. The NMR data of Fig. 10 clearly demonstrate that the 4′-OH groups of the tyramine and octopamine moieties are essentially free, indicating that they do not participate in coupling reactions and are not involved in forming ether linkages within the cell wall polymers. This indicates that tyramine and octopamine are essentially pendent terminal units. On the contrary, the NMR analysis also revealed that the 4-OH phenolic group of the ferulate moiety is predominantly bound (and is therefore not a free-phenolic-OH group), revealing that its phenolic group is largely involved in radical coupling reactions, forming ether linkages within the cell wall polymers.

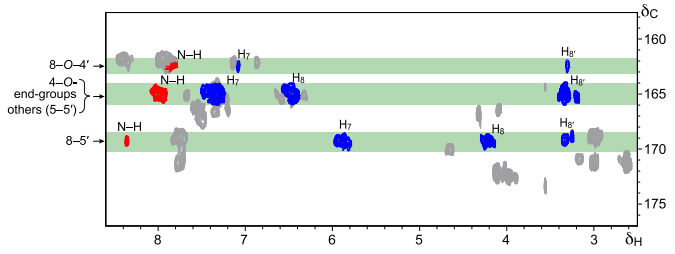

Fig. 9. Partial HMBC spectrum (δ_C 158–177) of the lignin/suberin-enriched fraction of potato periderms showing the correlations of the carbonyl carbon of the feruloyltyramine and feruloyloctopamine units with protons that are within three-bonds. Signals colored red correspond to the N–H correlations from the amide group, diagnostic for feruloyltyramine and feruloyloctopamine units in different structures.

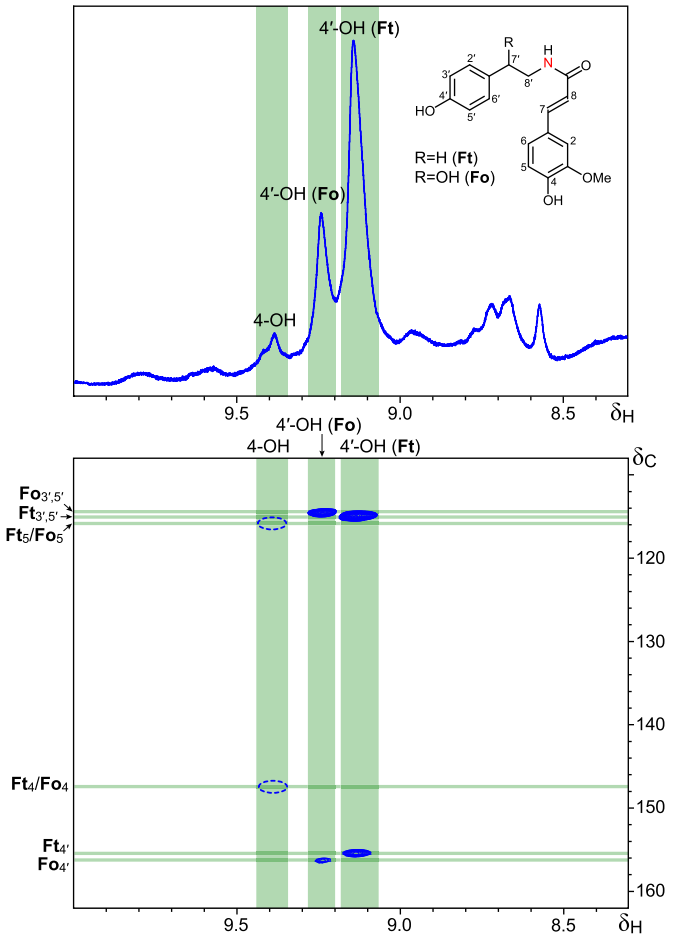

Fig. 10. Demonstration that the 4′-OH phenolic group of feruloyltyramine and feruloyloctopamine units remains largely free, and does not participate in ether linkages, whereas the 4-OH phenolic groups of the ferulate moieties are predominantly ether linked. (A) Partial ^{1}H NMR spectrum (δ_H 8.3–10.0) of the lignin/suberin-enriched fraction of potato periderms highlighting the characteristic signals corresponding to phenolic groups. (B) Partial HMBC spectrum (δ_C/δ_H 110–160/8.3–10.0) of lignin/suberin-enriched fraction from potato periderms, displaying correlation signals between the phenolic groups of the ferulate moiety (4-OH) and the phenolic groups of the tyramine, 4′-OH (**Ft**), and octopamine, 4′-OH (**Fo**), moieties.

This finding reinforces the conclusion that the feruloyltyramine and feruloyloctopamine moieties are covalently linked within the cell wall, with the tyramine and octopamine residues acting as terminal pendent groups, rather than existing as free molecules co-extracted during the isolation process of the lignin/suberin-enriched fraction.

Feruloyltyramine and feruloyloctopamine, along with some cross-linked dimers and trimers, have also been detected in free form in potato tubers, particularly in response to wounding or pathogen attack [50,51]. However, as the potato periderms examined in this study underwent exhaustive extraction with various solvents (dichloromethane, ethanol, water, and methanol) to remove free amides and other extractives before the isolation of the lignin/suberin-enriched fraction, and this fraction was further washed thoroughly with different organic solvents, it is reasonable to assume that the feruloyltyramine and feruloyloctopamine are covalently integrated into the cell walls, rather than being residual free molecules strongly associated with the cell walls. This assumption is also supported by GPC analysis of the isolated lignin/suberin fraction, as shown in Fig. 11, which indicated that it is polymeric and quite homogeneous (M_w of 4690 g/mol, M_n of 2300 g/mol, and with a very low polydispersity M_w/M_n of 2.0), and does not include free, non-polymerized ferulic acid amides that might have co-precipitated or co-extracted with the lignin/suberin-enriched fraction.

3.4. Role and biosynthesis of feruloyltyramine and feruloyloctopamine – prospects for lignin bioengineering

The periderm acts as the primary protective layer of potato tubers, with lignification and suberization playing a crucial role in enhancing this defense. Additionally, hydroxycinnamic acid amides are key contributors to plant development processes as well as plant responses against biotic and abiotic stress [52–54]. Among these metabolites, ferulic acid amides are particularly significant. Their polymerization within plant cell walls is widely recognized as a critical defense mechanism against pathogen invasion [26,27,32]. Beyond fortifying cell walls, ferulic acid amides impart antifungal and antimicrobial properties, playing a pivotal role in the plant's resistance to diseases and pathogen attack. By contributing to both physical defense and biochemical protection, these compounds are essential in safeguarding the plant, promoting a more resilient and disease-resistant plant structure.

The biosynthesis of feruloyltyramine and feruloyloctopamine involves two different metabolic routes leading to the formation of their parent compounds, ferulic acid on one side, and tyramine and octopamine on the other. Whereas ferulic acid arises from the shikimate-derived phenylpropanoid pathway, as do the monolignols, tyramine and octopamine are derived from the aromatic amino acid tyrosine by decarboxylation processes carried out by specific decarboxylase

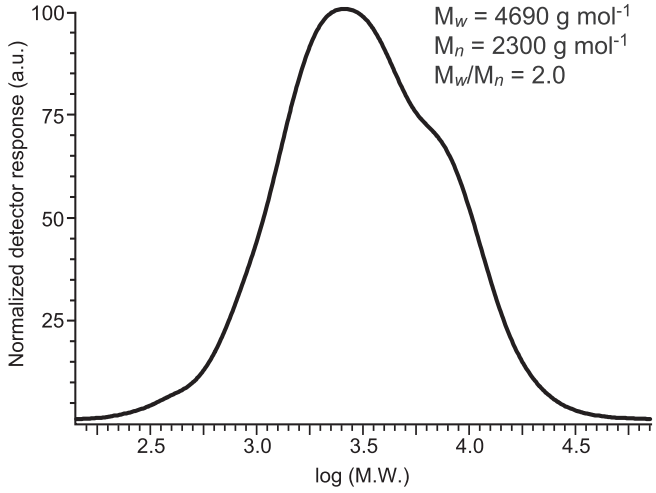

Fig. 11. GPC curve for the lignin/suberin-enriched fraction of potato periderms. The weight-average (M_w) molecular weight, number-average (M_n) molecular weight, and polydispersity index (M_w/M_n) are shown in the inset.

enzymes. These aromatic amino acid decarboxylases are type II pyridoxal phosphate-dependent decarboxylase enzymes that are responsive to abiotic and biotic stresses [55]. In plants, the biosynthesis of tyramine and octopamine begins with the conversion of tyrosine to tyramine by tyrosine decarboxylase (TYDC), followed by the transformation of tyramine into octopamine by tyramine β-hydroxylase (TβH) [52,54,56,57]. The condensation of feruloyl-CoA thioesters with tyramine and octopamine is then catalyzed by the feruloyl-CoA tyramine *N*-feruloyl-CoA transferase (THT) that is present in many plants, including potato tubers [58,59], and which presents similar affinity for both tyramine and octopamine [60].

On the other hand, it is important to note that the ferulic acid amides incorporated into the cell wall polymers of potato periderms are phenolic compounds compatible with the lignification process. Modifying the lignin to incorporate nontraditional monomers like feruloyltyramine and feruloyloctopamine, compounds not commonly found in native plant lignins, therefore opens exciting new possibilities in plant engineering. By using metabolic engineering to introduce these phenolic compounds into the lignin polymer, it is possible to precisely tailor its molecular architecture, potentially providing the lignin with enhanced physical and functional properties, as already considered with other phenolic compounds [61–63]. For instance, lignins modified with the introduction of feruloyltyramine and feruloyloctopamine may bolster plant defenses. Feruloyltyramine and feruloyloctopamine are known for their antifungal and antimicrobial properties, suggesting that their integration into lignin could enhance resistance of plants to diseases. Moreover, as these compounds contain nitrogen, their stable incorporation into lignin might also serve as a novel strategy to enrich soils with bioavailable nitrogen, potentially reducing the need for synthetic fertilizers. Overall, by redesigning lignin at the molecular level with these nonconventional monomers, we not only expand the functional versatility of this abundant biopolymer but also create opportunities for more sustainable agricultural and industrial practices.

4. Conclusions

The modes of incorporation of ferulic acid amides into the cell wall polymers of potato periderms has been investigated. A lignin/suberin-enriched fraction was isolated and analyzed using DFRC, NMR, and GPC techniques. The lignin was found to be predominantly composed of G-lignin units, with an H:G:S ratio of 2:70:28 (SG ratio of 0.40). Additionally, significant amounts of feruloyltyramine and feruloyloctopamine were detected as being incorporated. These compounds participate in radical coupling reactions and form various cross-linkages within the cell wall, including via 8–*O*- and 4–*O*-ether linkages, as well as 8–5 linkages leading to the formation of phenylcoumaran structures. Interestingly, although most of the 4-OH phenolic groups of the ferulate moieties were involved in ether linkages within the polymer, indicating their participation in radical coupling reactions, the 4′-OH phenolic groups of the tyramine and octopamine moieties remained largely free, suggesting they act as terminal pendent units and were not involved in radical coupling reactions. Finally, as ferulic acid amides are compatible with lignification, these compounds offer promising opportunities for the genetic engineering of plants to incorporate them into their lignins, potentially leading to polymers with unique and specialized properties such as improved plant resistance to pathogens or increased bioavailability of nitrogen in soils.

CRediT authorship contribution statement

José C. del Río: Writing – original draft, Resources, Project administration, Methodology, Funding acquisition, Data curation, Conceptualization. **John Ralph:** Writing – review & editing. **José J. Benítez:** Resources, Methodology, Funding acquisition. **Susana Guzman-Puyol:** Resources, Methodology. **José A. Heredia-Guerrero:** Resources, Methodology, Funding acquisition. **Jorge Rencoret:** Writing – review & editing, Resources, Methodology, Formal analysis, Data curation, Conceptualization.

Funding

This research was supported by project PID2023-152543OB-I00, funded by the Spanish MICIU/AEI/10.13039/501100011033 and the European Regional Development Fund (ERDF) "A way of making Europe," as well as project TED2021-129656B-I00, funded by the Spanish MICIU/AEI/10.13039/501100011033 and the European Union's "NextGenerationEU"/PRTR initiative. JR was supported by the Great Lakes Bioenergy Research Center, U.S. Department of Energy, Office of Science, Biological and Environmental Research Program under Award Number DE-SC0018409.

Declaration of competing interest

The authors declare that they have no known competing financial interests or personal relationships that could have appeared to influence the work reported in this paper.

Acknowledgements

The authors thank "El Tío de las Papas S.L." for kindly providing the potato peels used in this study. We extend our gratitude to Dr. Manuel Angulo from SGI-CITIUS, University of Seville, for his assistance in acquiring the NMR spectra.

References

[1] W. Boerjan, J. Ralph, M. Baucher, Lignin biosynthesis, Annu. Rev. Plant Biol. 54 (2003) 519–546, https://doi.org/10.1146/annurev.arplant.54.031902.134938.
[2] J. Ralph, K. Lundquist, G. Brunow, F. Lu, H. Kim, P.F. Schatz, J.M. Marita, R. D. Hatfield, S.A. Ralph, J.H. Christensen, W. Boerjan, Lignins: natural polymers from oxidative coupling of 4-hydroxyphenylpropanoids, Phytochem. Rev. 3 (2004) 29–60, https://doi.org/10.1023/B:PHYT.0000047809.65444.a4.
[3] J. Ralph, C. Lapierre, W. Boerjan, Lignin structure and its engineering, Curr. Opin. Biotechnol. 56 (2019) 240–249, https://doi.org/10.1016/j.copbio.2019.02.019.
[4] R. Vanholme, B. Demedts, K. Morreel, J. Ralph, W. Boerjan, Lignin biosynthesis and structure, Plant Physiol. 153 (2010) 895–905, https://doi.org/10.1104/pp.110.155119.
[5] R. Vanholme, B. De Meester, J. Ralph, W. Boerjan, Lignin biosynthesis and its integration into metabolism, Curr. Opin. Biotechnol. 56 (2019) 230–239, https://doi.org/10.1016/j.copbio.2019.02.018.
[6] J.V. Vermaas, R.A. Dixon, F. Chen, S.D. Mansfield, W. Boerjan, J. Ralph, M. F. Crowley, G.T. Beckham, Passive membrane transport of lignin-related compounds, Proc. Natl. Acad. Sci. USA 116 (2019) 23117–23123, https://doi.org/10.1073/pnas.1904643116.
[7] J. Ralph, Hydroxycinnamates in lignification, Phytochem. Rev. 9 (2010) 65–83, https://doi.org/10.1007/s11101-009-9141-9.
[8] S.D. Karlen, R.A. Smith, H. Kim, D. Padmakshan, A. Bartuce, J.K. Mobley, H.C. A. Free, B.G. Smith, P.J. Harris, J. Ralph, Highly decorated lignins occur in leaf base cell walls of the Canary Island date palm *Phoenix canariensis*, Plant Physiol. 175 (2017) 1058–1067, https://doi.org/10.1104/pp.17.01172.
[9] J.C. del Río, J. Rencoret, G. Marques, A. Gutiérrez, D. Ibarra, J.I. Santos, J. Jiménez-Barbero, L. Zhang, A.T. Martínez, Highly acylated (acetylated and/or *p*-coumaroylated) native lignins from diverse herbaceous plants, J. Agric. Food Chem. 56 (2008) 9525–9534, https://doi.org/10.1021/jf800806h.
[10] J.C. del Río, J. Rencoret, A. Gutiérrez, H. Kim, J. Ralph, Unconventional lignin monomers – extension of the lignin paradigm, Adv. Bot. Res. 104 (2022) 1–39, https://doi.org/10.1016/bs.abr.2022.02.001.
[11] J. Ralph, H. Kim, F. Lu, R.A. Smith, S.D. Karlen, K. Yoshioka Nuoendagula, A. Eugene, S. Liu, C. Sener, D. Ando, M.J. Chen, Y. Li, L.L. Landucci, S.A. Ralph, V. I. Timokhin, W. Lan, J. Rencoret, J.C. del Río, Lignins and lignification: New developments and emerging concepts, in: S. Quideau, J.P. Salminen, K. Wähälä, V. de Freitas (Eds.), Recent Advances in Polyphenol Research 8, Wiley-Blackwell Publishing, Oxford, UK, 2023, pp. 1–50, https://doi.org/10.1002/9781119844792.ch1.
[12] J.C. del Río, J. Rencoret, A. Gutiérrez, T. Elder, H. Kim, J. Ralph, Lignin monomers from beyond the canonical monolignol biosynthetic pathway: another brick in the wall, ACS Sustain. Chem. Eng. 8 (2020) 4997–5012, https://doi.org/10.1021/acssuschemeng.0c01109.
[13] J.C. del Río, J. Rencoret, A. Gutiérrez, W. Lan, H. Kim, J. Ralph, Lignin monomers derived from the flavonoid and hydroxystilbene biosynthetic pathways, in: J. D. Reed, V.A.P. de Freitas, S. Quideau (Eds.), Recent Advances in Polyphenol Research vol. 7, Wiley-Blackwell Publishing, Oxford, UK, 2021, pp. 177–206, https://doi.org/10.1002/9781119545958.ch7.

[14] J.C. del Río, J. Rencoret, P. Prinsen, A.T. Martínez, J. Ralph, A. Gutiérrez, Structural characterization of wheat straw lignin as revealed by analytical pyrolysis, 2D-NMR, and reductive cleavage methods, J. Agric. Food Chem. 60 (2012) 5922–5935, https://doi.org/10.1021/jf301002n.
[15] J.C. del Río, A.G. Lino, J.L. Colodette, C.F. Lima, A. Gutiérrez, A.T. Martínez, F. Lu, J. Ralph, J. Rencoret, Differences in the chemical structures of the lignins from sugarcane bagasse and straw, Biomass Bioenergy 81 (2015) 322–338, https://doi.org/10.1016/j.biombioe.2015.07.006.
[16] W. Lan, F. Lu, M. Regner, Y. Zhu, J. Rencoret, S.A. Ralph, U.I. Zakai, K. Morreel, W. Boerjan, J. Ralph, Tricin, a flavonoid monomer in monocot lignification, Plant Physiol. 167 (2015) 1284–1295, https://doi.org/10.1104/pp.114.253757.
[17] W. Lan, K. Morreel, F. Lu, J. Rencoret, J.C. del Río, W. Vooren, W. Vermerris, W. Boerjan, J. Ralph, Maize tricin-oligolignol metabolites and their implications for monocot lignification, Plant Physiol. 171 (2016) 810–820, https://doi.org/10.1104/pp.16.02012.
[18] W. Lan, J. Rencoret, F. Lu, S. Karlen, B.G. Smith, P.J. Harris, J.C. del Río, J. Ralph, Tricin-lignins: occurrence and quantitation of tricin in relation to phylogeny, Plant J. 88 (2016) 1046–1057, https://doi.org/10.1111/tpj.13315.
[19] M.J. Rosado, J. Rencoret, G. Marques, A. Gutiérrez, J.C. del Río, Structural characteristics of the guaiacyl-rich lignins from rice (*Oryza sativa* L.) husks and straw, Front. Plant Sci. 12 (2021) 640475, https://doi.org/10.3389/fpls.2021.640475.
[20] M.J. Rosado, F. Bausch, J. Rencoret, G. Marques, A. Gutiérrez, T. Rosenau, A. Potthast, J.C. del Río, Differences in content, composition and structure of the lignins from the rind and pith of papyrus (*Cyperus papyrus* L.) culms, Ind. Crop Prod. 174 (2021) 114226, https://doi.org/10.1016/j.indcrop.2021.114226.
[21] J. Rencoret, M.J. Rosado, H. Kim, V. Tymokhin, A. Gutiérrez, F. Bausch, T. Rosenau, A. Potthast, J. Ralph, J.C. del Río, Flavonoids naringenin chalcone, naringenin, dihydrotricin, and tricin are lignin monomers in papyrus, Plant Physiol. 188 (2022) 208–2019, https://doi.org/10.1093/plphys/kiab469.
[22] J.C. del Río, J. Rencoret, A. Gutiérrez, H. Kim, J. Ralph, Hydroxystilbenes are monomers in palm fruit endocarp lignins, Plant Physiol. 174 (2017) 2072–2082, https://doi.org/10.1104/pp.17.00362.
[23] J. Rencoret, H. Kim, A.B. Evaristo, A. Gutiérrez, J. Ralph, J.C. del Río, Variability in lignin composition and structure in cell walls of different parts of macaúba (*Acrocomia aculeata*) palm fruit, J. Agric. Food Chem. 66 (2018) 138–153, https://doi.org/10.1021/acs.jafc.7b04638.
[24] J. Rencoret, D. Neiva, G. Marques, A. Gutiérrez, H. Kim, J. Gominho, H. Pereira, J. Ralph, J.C. del Río, Hydroxystilbene glucosides are incorporated into Norway spruce bark lignin, Plant Physiol. 180 (2019) 1310–1321, https://doi.org/10.1104/pp.19.00344.
[25] D. Neiva, J. Rencoret, G. Marques, A. Gutiérrez, J. Gominho, H. Pereira, J.C. del Río, Lignin from tree barks: chemical structure and valorization, ChemSusChem 13 (2020) 4537–4547, https://doi.org/10.1002/cssc.202000431.
[26] J. Negrel, B. Pollet, C. Lapierre, Ether-linked ferulic acid amides in natural and wound periderms of potato tuber, Phytochemistry 43 (1996) 1195–1199, https://doi.org/10.1016/S0031-9422(96)00500-6.
[27] J. Negrel, P. Jeandet, Metabolism of tyramine and feruloyltyramine in TMV inoculated leaves of *Nicotiana tabacum*, Phytochemistry 26 (1987) 2185–2190, https://doi.org/10.1016/S0031-9422(00)84681-6.
[28] J. Negrel, F. Javelle, Induction of phenylpropanoid and tyramine metabolism in pectinase- or pronase-elicited cell suspension cultures of tobacco (*Nicotiana tabacum*), Physiol. Plant. 95 (1995) 569–574, https://doi.org/10.1111/j.1399-3054.1995.tb05524.x.
[29] J. Ralph, R.D. Hatfield, J. Piquemal, N. Yahiaoui, M. Pean, C. Lapierre, A. M. Boudet, NMR characterization of altered lignins extracted from tobacco plants down-regulated for lignification enzymes cinnamyl-alcohol dehydrogenase and cinnamoyl-CoA reductase, Proc. Natl. Acad. Sci. USA 95 (1998) 12803–12808, https://doi.org/10.1073/pnas.95.22.12803.
[30] H. Kaur, K. Shaker, N. Heinzel, J. Ralph, I. Gális, I.T. Baldwin, Environmental stresses of field growth allow cinnamyl alcohol dehydrogenase-deficient *Nicotiana attenuata* plants to compensate for their structural deficiencies, Plant Physiol. 159 (2012) 1545–1570, https://doi.org/10.1104/pp.112.196717.
[31] Y. Joo, H. Kim, M. Kang, G. Lee, S. Choung, H. Kaur, S. Oh, J.W. Choi, J. Ralph, I. T. Baldwin, S.-G. Kim, Pith-specific lignification in *Nicotiana attenuata* as a defense against a stem-boring herbivore, New Phytol. 232 (2021) 332–344, https://doi.org/10.1111/nph.17583.
[32] A. Kashyap, A.L. Jiménez-Jiménez, W. Zhang, M. Capellades, S. Srinivasan, A. Laromaine, O. Serra, M. Figueras, J. Rencoret, A. Gutiérrez, M. Valls, N.S. Coll, Induced ligno-suberin vascular coating and tyramine-derived hydroxycinnamic acid amides restrict *Ralstonia solanacearum* colonization in resistant tomato, New Phytol. 234 (2022) 1411–1429, https://doi.org/10.1111/nph.17982.
[33] J.C. del Río, J. Rencoret, A. Gutiérrez, H. Kim, J. Ralph, Structural characterization of lignin from maize (*Zea mays* L.) fibers: evidence for diferuloylputrescine incorporated into the lignin polymer in maize kernels, J. Agric. Food Chem. 66 (2018) 4402–4413, https://doi.org/10.1021/acs.jafc.8b00880.
[34] O. Borg-Olivier, B. Monties, Lignin, suberin, phenolic acids and tyramine in the suberized, wound-induced potato periderm, Phytochemisty 32 (1993) 601–606, https://doi.org/10.1016/S0031-9422(00)95143-4.
[35] M.A. Bernards, M.L. Lopez, J. Zajicek, N.G. Lewis, Hydroxycinnamic acid-derived polymers constitute the polyaromatic domain of suberin, J. Biol. Chem. 270 (1995) 7382–7386, https://doi.org/10.1074/jbc.270.13.7382.
[36] J. Graça, Hydroxycinnamates in suberin formation, Phytochem. Rev. 9 (2009) 85–91, https://doi.org/10.1007/s11101-009-9138-4.
[37] J.C. del Río, P. Prinsen, J. Rencoret, L. Nieto, J. Jiménez-Barbero, J. Ralph, A. T. Martínez, A. Gutiérrez, Structural characterization of the lignin in the cortex and pith of elephant grass (*Pennisetum purpureum*) stems, J. Agric. Food Chem. 60 (2012) 3619–3634, https://doi.org/10.1021/jf300099g.
[38] F. Lu, J. Ralph, Derivatization followed by reductive cleavage (DFRC method), a new method for lignin analysis: protocol for analysis of DFRC monomers, J. Agric. Food Chem. 45 (1997) 2590–2592, https://doi.org/10.1021/jf970258h.
[39] C. Lapierre, B. Pollet, J. Negrel, The phenolic domain of potato suberin: structural comparison with lignins, Phytochemistry 42 (1996) 949–953, https://doi.org/10.1016/0031-9422(96)00097-0.
[40] M. Regner, A. Bartuce, D. Padmakshan, J. Ralph, S.D. Karlen, Reductive cleavage method for quantitation of monolignols and low-abundance monolignol conjugates, ChemSusChem 11 (2018) 1600–1605, https://doi.org/10.1002/cssc.201800617.
[41] F. Lu, J. Ralph, Efficient ether cleavage in lignins: The derivatization followed by reductive cleavage procedure as a basis for new analytical methods, in: N.G. Lewis, S. Sarkanen (Eds.), Lignin and Lignan Biosynthesis, American Chemical Society, Washington DC, 1998, pp. 294–322, https://doi.org/10.1021/bk-1998-0697.ch020.
[42] J. Ralph, F. Lu, The DFRC method for lignin analysis. Part 6. A simple modification for identifying natural acetates on lignins, J. Agric. Food Chem. 46 (1998) 4616–4619, https://doi.org/10.1021/jf980680d.
[43] F. Lu, J. Ralph, Detection and determination of *p*-coumaroylated units in lignins, J. Agric. Food Chem. 47 (1999) 1988–1992, https://doi.org/10.1021/jf981140j.
[44] P. Karhunen, P. Rummakko, J. Sipilä, G. Brunow, I. Kilpeläinen, Dibenzodioxocins; a novel type of linkage in softwood lignins, Tetrahedron Lett. 36 (1995) 169–170, https://doi.org/10.1016/0040-4039(94)02203-N.
[45] L. Cseri, S. Kumar, P. Palchuber, G. Szekely, NMR chemical shifts of emerging green solvents, acids, and bases for facile trace impurity analysis, ACS Sustain. Chem. Eng. 11 (2023) 5696–5725, https://doi.org/10.1021/acssuschemeng.3c00244.
[46] J. Ralph, S. Quideau, J.H. Grabber, R.D. Hatfield, Identification and synthesis of new ferulic acid dehydrodimers present in the grass cell walls, J. Chem. Soc. Perkin Trans. 1 (1994) 3485–3498, https://doi.org/10.1039/P19940003485.
[47] A. Zhang, F. Lu, R. Sun, J. Ralph, Ferulate-coniferyl alcohol cross-coupled products formed by radical coupling reactions, Planta 229 (2009) 1099–1108, https://doi.org/10.1007/s00425-009-0894-6.
[48] J. Ralph, J.H. Grabber, R.D. Hatfield, Lignin-ferulate cross-links in grasses: active incorporation of ferulate polysaccharide esters in ryegrass lignins, Carbohydr. Res. 275 (1995) 167–178, https://doi.org/10.1016/0008-6215(95)00237-N.
[49] S. Quideau, J. Ralph, Lignin-ferulate cross-links in grasses. Part 4. Incorporation of 5–5-coupled dehydrodiferulate into synthetic lignin, J. Chem. Soc. Perkin Trans. 1 (1997) 2351–2358, https://doi.org/10.1039/A701808H.
[50] R.R. King, L.A. Calhoun, Characterization of cross-linked hydroxycinnamic acid amides isolated from potato common scab lesions, Phytochemistry 66 (2005) 2468–2473, https://doi.org/10.1016/j.phytochem.2005.07.014.
[51] R.R. King, L.A. Calhoun, A feruloyltyramine trimer isolated from potato common scab lesions, Phytochemistry 71 (2010) 2187–2189, https://doi.org/10.1016/j.phytochem.2010.09.020.
[52] P.J. Facchini, K.L. Huber-Allanach, L.W. Tari, Plant aromatic L-amino acid decarboxylases: evolution, biochemistry, regulation, and metabolic engineering applications, Phytochemistry 54 (2000) 121–138, https://doi.org/10.1016/s0031-9422(00)00050-9.
[53] A.M. Edreva, V.B. Velikova, T.D. Tsonev, Phenylamides in plants, Russ. J. Plant Physiol. 54 (2007) 278–301, https://doi.org/10.1134/S1021443707030016.
[54] D.N. Macoy, W.-Y. Kim, S.Y. Lee, M.G. Kim, Biosynthesis, physiology, and functions of hydroxycinnamic acid amides in plants, Plant Biotechnol. Rep. 9 (2015) 269–278, https://doi.org/10.1007/s11816-015-0368-1.
[55] J.-E. Bassard, P. Ullmann, F. Bernier, D. Werck-Reichhart, Phenolamides: bridging polyamines to the phenolic metabolism, Phytochemistry 71 (2010) 1808–1824, https://doi.org/10.1016/j.phytochem.2010.08.003.
[56] K. Lee, K. Kang, M. Park, S. Park, K. Back, Enhanced octopamine synthesis through the ectopic expression of tyrosine decarboxylase in rice plants, Plant Sci. 176 (2009) 46–50, https://doi.org/10.1016/j.plantsci.2008.09.006.
[57] J. Feng, R. Jin, S. Cheng, H. Li, X. Wang, K. Chen, Establishing an artificial pathway for the biosynthesis of octopamine and synephrine, ACS Synth. Biol. 13 (2024) 1762–1772, https://doi.org/10.1021/acssynbio.4c00082.
[58] J. Negrel, F. Javelle, M. Paynot, Wood-induced tyramine hydroxycinnamoyl transferase in potato (*Solanum tuberosum*) tuber disks, J. Plant Physiol. 142 (1993) 518–524, https://doi.org/10.1016/S0176-1617(11)80392-5.
[59] A. Schmidt, R. Grimm, J. Schmidt, D. Scheel, D. Strack, S. Roshal, Cloning and expression of a potato cDNA encoding hydroxycinnamoyl-CoA:tyramine *N*-(hydroxycinnamoyl) transferase, J. Biol. Chem. 274 (1999) 4273–4280, https://doi.org/10.1074/jbc.274.7.4273.
[60] J. Negrel, C. Martin, The biosynthesis of feruloyltyramine in *Nicotiana tabacum*, Phytochemistry 23 (1984) 2797–2801, https://doi.org/10.1016/0031-9422(84)83018-6.
[61] R. Vanholme, K. Morreel, J. Ralph, W. Boerjan, Lignin engineering, Curr. Opin. Plant Biol. 11 (2008) 278–285, https://doi.org/10.1016/j.pbi.2008.03.005.
[62] R. Vanholme, K. Morreel, C. Darrah, P. Oyarce, J.H. Grabber, J. Ralph, W. Boerjan, Metabolic engineering of novel lignin in biomass crops, New Phytol. 196 (2012) 978–1000, https://doi.org/10.1111/j.1469-8137.2012.04337.x.
[63] Y. Mottiar, R. Vanholme, W. Boerjan, J. Ralph, S.D. Mansfield, Designer lignins: harnessing the plasticity of lignification, Curr. Opin. Biotechnol. 37 (2016) 190–200, https://doi.org/10.1016/j.copbio.2015.10.009.